APEC: Auto Planner for Efficient Configuration of Indoor Positioning System

Ming Jin, Ruoxi Jia, Costas J. Spanos

Department of Electrical Engineering and Computer Science
University of California, Berkeley
Berkeley, CA 94720, USA
Emails: {jinming,ruoxijia,spanos}@berkeley.edu

***Abstract*—Fingerprints-based methods have been prevailing in indoor positioning systems, whereas they have certain drawbacks that fingerprints collection in the offline phase requires considerable manpower and time. Auto Planner for Efficient Configuration (APEC) systematically exploits router setups and fingerprints allocations over space by taking into account user preferences and budget constraints. The task of configuration is formulated as an optimization problem, whose objective is the expected loss based on the Hierarchical Bayesian Signal Model (HBSM) and theoretical results on the misclassification rates. To reduce the computational complexity of large-scale problems, two heuristics are employed, i.e., *the coordinate descent* and the *router-fingerprints decoupling*, which are validated by simulation analysis. Experiments with three mobile devices (Android, iPad, iPhone) in two setups (7 or 9 access points) verify that the expected loss is a reliable predictor of the actual loss of the system (*objective consistency*), and that APEC outperforms the random and uniform approaches (*solution superiority*). Since APEC focuses on the system configuration in the planning stage, it can be combined with other fingerprinting processes in the online phase to improve the utility of the system.**

Keywords–Indoor positioning; Fingerprinting method; System optimization

I. Introduction

The pervasion of radio-frequency transmitters such as WiFi access points, iBeacons and GSM towers has gathered momentum for indoor positioning without the need for specialized infrastructure. One popular approach, pioneered by RADAR [1] and further developed by [2]–[7], is to employ received signal strength (RSS) based fingerprinting of locations in the space of interest, where typically multiple access points can be heard at each location. A mobile device is then localized by matching the observed RSS readings against the database by deterministic, e.g., K-Nearest Neighbors (KNN), or stochastic methods, e.g., maximum likelihood criterion. While the fingerprinting approach requires a site survey involving detailed RSS measurements which entail considerable effort, an alternative method is to use RF propagation model, such as the prevalent log-distance pass-loss model, which leads to light-weighted localization schemes [8]–[11]. Model-based localization method itself suffers from reduced accuracy since the model can hardly capture signal variance resulting from complexities of indoor environments. The combination of fingerprinting and model-based methods has been proposed as a trade-off between accuracy and RSS measurement effort, such as [12], [13].

Previous work has been devoting effort to maneuvering fingerprinting matching process in the online phase to achieve better localization accuracy, while it remains untouched that potential performance improvement can be obtained by exploiting an optimized way to collect fingerprints in the offline phase. The focus of this study is on the configuration of fingerprints-based positioning system as motivated by the following problems:

- How to take user preferences, i.e., location priority and visiting frequencies, into account?
- How to place routers and allocate fingerprints to be collected over the space under budget constraints?

The first problem arises, for instance, in the scenarios such as: (i) customer behavior analysis in a supermarket, where merchandise area has higher priority than check-out stations, or (ii) region-based indoor environment control, where climate zones are more important than open spaces. The second problem emerges since router setup involves capital costs and fingerprints collection is time-consuming.

It is, therefore, the objective of the APEC *to design the fingerprints-based localization system that takes into account user preferences and budget constraints.* The key contributions of the study are as follow:

- Proposal of Hierarchical Bayesian Signal Model (HBSM), a learning-to-learn framework to improve RSSI estimation over space.
- Formulation of the optimization problem, where the objective as a theoretical solution has strong correlation with the actual loss of the system.
- Design and implementation of APEC as a guidance for field deployments.

The rest of the paper is organized as follow. The HBSM is detailed in Section II. Section III formulates the optimization problem and derives the expected loss based on linear/quadratic discriminant analysis, followed by the illustration of the APEC algorithm. Results of field experiments are reported in Section IV, in addition to a toy example to examine the heuristics and algorithmic performances. Section V draws conclusion and discusses future works. Notations and shorthands in the paper are listed in Table I as a reference.

II. Hierarchical Bayesian Signal Model

A. Background

1) Log-Distance Pass-Loss Model: The path loss of signal strength inside a building over distance is modeled as

$$X^{\text{RSSI}}(d) = X^{\text{RSSI}}(d_0) + 10\gamma \log \frac{d}{d_0} + \epsilon_\sigma, \qquad (1)$$

TABLE I. NOTATIONS AND SHORTHANDS REFERENCE.

Random variables	
$X^{RSSI}(d)$	RSSI at distance d by log-distance pass-loss model
ϵ_σ	Random variable with $\epsilon_\sigma \sim \mathcal{N}(0, \sigma^2)$
$Z \sim P_Z$	Location Z follows the visiting frequency probability P_Z
$X \sim P_{X\|Z}$	RSSI measurement X at location Z distributed as $P_{X\|Z}$
$\boldsymbol{x}_i^{(t)}$	RSSI measurement at location i and time t, which is the realization of $X \sim \mathcal{N}(\Lambda_{i,\cdot}^\top, \tilde{\Sigma}_i)$
Parameters	
K	Total number of routers
N	Number of subregions
M	Number of places available for routers
N_{tot}	Total number of fingerprints to be collected
$\boldsymbol{\theta}=\{\boldsymbol{\theta}^{fp},\boldsymbol{\theta}^{rt}\}$	fingerprints allocation parameter $\boldsymbol{\theta}^{fp} \in \mathcal{N}_+^N$ and router location parameter $\boldsymbol{\theta}^{fp} \in \mathbb{R}^M$
S^{rt}	Set of possible location candidates for $\boldsymbol{\theta}^{rt}$
$n_i, \boldsymbol{\theta}_i^{fp}$	Number of fingerprints collected at location $i \in [N]$
$\Lambda \in \mathbb{R}^{N\times K}$	Mean matrix, with $\Lambda_{i,\cdot}$ for mean RSSI at location $i \in [N]$ and $\Lambda_{\cdot,j}$ for all location measurements for router $j \in [K]$
$\tilde{\Sigma}_i$	Covariance matrix for RSSI measurement at location i
$\tilde{\Sigma}, \tilde{\sigma}^2$	$\tilde{\sigma}^2$ is the diagonal entry of RSSI covariance matrix $\tilde{\Sigma}$, which by assumption is the same for all $\tilde{\Sigma}_i$, $i \in [N]$
Σ_{ml}, s_{ml}	$\Sigma_{ml} = \Sigma_m^{-1} - \Sigma_l^{-1}$ whose diagonal entries are identically s_{ml} in Section III-B2 QDA misclassification
$\tilde{\Lambda} \in \mathbb{R}^{N\times K}$ $\tilde{\Gamma} \in \mathbb{R}^{NK\times NK}$	Hyperpriors of Λ, $\Lambda_{\cdot,j} \sim \mathcal{N}(\tilde{\Lambda}_{\cdot,j}, \tilde{\Gamma}_{\beta(j)})$ for router j and $\Lambda_{i,\cdot}^\top \sim \mathcal{N}(\tilde{\Lambda}_{i,\cdot}^\top, \tilde{\Gamma}_{\alpha(i)})$ for location i
$\boldsymbol{c} \in \mathbb{R}^N$	local priority map, $\boldsymbol{c}_i \in$ {HIGH, MED, LOW} for location i
$\boldsymbol{\pi} \in \mathbb{R}^N$	local frequency map, $\boldsymbol{\pi}_i \in$ {OFTEN, SOME, SELDOM}
Shorthand notations and functions	
$[K]$	Shorthand notation for $\{1, ..., K\}$
$R(i)$	Neighborhood of location i
$\alpha(i)$ index func.	$\{(x, y) : x = i+pN, y = i+qN, p, q \in \{0, ..., K-1\}\}$
$\beta(j)$ index func.	$\{(x, y) : (j-1)N + 1 \le x, y \le jN\}$
$h_{\boldsymbol{\theta}}(\boldsymbol{x})$	Output of IPS parameterized by $\boldsymbol{\theta}$ given RSSI $\boldsymbol{x}$
$L(Z, \hat{Z})$	Cost of misclassification given the target is at Z, as in (3)
$P_m(h(\boldsymbol{x}) \neq m)$	Misclassification rate of $h(\cdot)$ given $\boldsymbol{x}$ and true location m
$\hat{L}(\boldsymbol{\theta}^{rt}, \boldsymbol{\theta}^{fp})$	Actual loss of an IPS designed by $(\boldsymbol{\theta}^{rt}, \boldsymbol{\theta}^{fp})$ as in (12)
$\xi_i(j)$	Empirical misclassification rate of location i to j (13)

where $X^{\text{RSSI}}(d)$ in Decibel (dB) is the received signal strength indicator (RSSI) at distance d, d_0 is the reference distance, γ is the path loss exponent (PLE), and $\epsilon_\sigma \sim \mathcal{N}(0, \sigma^2)$ is a random variable reflecting the attenuation caused by flat fading.

2) Gaussian Process (GP): Every point in space has a normal distribution by the Gaussian process. A collection of points follows a multivariate Gaussian, $\boldsymbol{x} \sim \mathcal{N}(\boldsymbol{\mu}, \tilde{\Sigma})$ that is characterized by $\boldsymbol{\mu}$ and $\tilde{\Sigma}$ given by the mean and covariance functions respectively. GP has been employed in spatial smoothing, aka kriging, and prediction. The covariance function can take many forms, such as constant ($K_C(\boldsymbol{z}, \boldsymbol{z}') = C$), Gaussian noise ($K_{GN}(\boldsymbol{z}, \boldsymbol{z}') = \sigma^2 \delta_{\boldsymbol{z},\boldsymbol{z}'}$), and squared exponential $\left(K_{SE} = \exp\{-\frac{\|\boldsymbol{z}-\boldsymbol{z}'\|_2^2}{2}\}\right)$, where $\boldsymbol{z}$ and $\boldsymbol{z}'$ are spatial positions of any two points.

We propose a neighborhood covariance function, $K_{NH} = \rho\sigma^2 \delta_{\boldsymbol{z}\in R(\boldsymbol{z}')}$, where $R(\boldsymbol{z})$ is a set of points that are in the neighborhood of $\boldsymbol{z}$, $\rho \in (0, 1)$ is the GP coefficient, and $\delta_{\boldsymbol{z}\in R(\boldsymbol{z}')}$ is an indicator function which evaluates to 1 if $\boldsymbol{z}$ is in the neighborhood of $R(\boldsymbol{z}')$ and 0 otherwise. The neighborhood covariance is symmetric, and by appropriate choice of ρ, positive definite.

B. Hierarchical Bayesian Signal Model (HBSM)

The space is instrumented with K routers, each of which can independently produce RSSI measurements within the area. The HBSM proposed in this study is a two-layered model for the RSSI observations. The top layer imposes hyperpriors on the mean of RSSI at any point, whereas the bottom layer accounts for measurement error.

*1) **Bottom layer (observations)**:* Let $\boldsymbol{x}_i^{(t)} \in \mathbb{R}^K$ denote measurement at location $i \in [N]$ and time t for K routers. $\boldsymbol{x}_i^{(t)} \sim \mathcal{N}(\Lambda_{i,\cdot}^\top, \tilde{\Sigma}_i)$ follows a normal distribution with mean $\Lambda_{i,\cdot}^\top$ and covariance $\tilde{\Sigma}_i$, where $\Lambda \in \mathbb{R}^{N\times K}$ is the **mean matrix** whose i-th row corresponds to the mean RSSI at location $i \in [N]$ and j-th column corresponds to all location measurements for router $j \in [K]$, where we use notations with tilde to represent hyperpriors, which are non random and can be estimated by sample averages. The signal can be considered as a summation of the mean signal $\Lambda \in \mathbb{R}^{N\times K}$ with a multivariate Gaussian random noise $\epsilon_t \sim \mathcal{N}(0, \tilde{\Sigma}_i)$, which results from randomness of measurement and environments. We make the following assumption of the system:

Assumption 1: Routers work independently and identically, which, by the log-distance pass-loss model (1), indicates that $\tilde{\Sigma}_i = \tilde{\Sigma}$, $i \in [N]$, with identical diagonal entries $\tilde{\sigma}^2$.

*2) **Top layer (hyperpriors)**:* The rearranged mean matrix $\begin{bmatrix} \Lambda_{\cdot,1} \\ \vdots \\ \Lambda_{\cdot,K} \end{bmatrix} \sim \mathcal{N}\left(\begin{bmatrix} \tilde{\Lambda}_{\cdot,1} \\ \vdots \\ \tilde{\Lambda}_{\cdot,K} \end{bmatrix}, \tilde{\Gamma} = \begin{bmatrix} \tilde{\Gamma}_{\beta(1)} & & \\ & \ddots & \\ & & \tilde{\Gamma}_{\beta(K)} \end{bmatrix} \right)$ has multivariate Gaussian distribution, where $\tilde{\Lambda} \in \mathbb{R}^{N\times K}$ is the mean and $\tilde{\Gamma}$ is the covariance matrix. We introduce the indexing functions:

$$\alpha(i) = \{(x, y) : x = i+pN, y = i+qN, p, q \in \{0, ..., K-1\}\}$$
$$\beta(j) = \{(x, y) : (j-1)N + 1 \le x, y \le jN\}$$

where $\alpha(i)$ and $\beta(j)$ extracts the covariance terms from $\tilde{\Gamma}$ for location i and router j, respectively. By rearranging the terms we have $\Lambda_{i,\cdot}^\top \sim \mathcal{N}(\tilde{\Lambda}_{i,\cdot}^\top, \tilde{\Gamma}_{\alpha(i)})$ as can be verified.

Assumption 2: The mean of the hyperprior, $\tilde{\Lambda}$, is given by the log-distance pass-loss model. The diagonal variance and off-diagonal covariance for all locations corresponding to a single router j, $\tilde{\Gamma}_{\beta(j)}$, is given by the log-distance pass-loss model and Gaussian process model respectively.

Remarks: The HBSM model is inspired by the learning to learn framework [14], where the observation at one point in space can refine our estimation of other points through the top layer of hyperpriors. It lays the theoretical foundation of many empirically proven fingerprinting methods, such as Virtual Fingerprints [15], Modellet [13] and CGSIL [16], where the collected fingerprints are used to train a radio propagation model locally in order to estimate the unknown area. The HBSM model also has implications to radio map reconstruction by introducing methods from empirical Bayes and Gaussian process regressions [17].

III. Auto Planner for Efficient Configuration

We describe the APEC framework in this section. The key idea is that given limited resources (routers and fingerprints), critical locations that are visited frequently should be distinguished with high accuracy. APEC requires users to provide two maps as illustrated in Figures 1 and 7 in the Experiment section (Section IV-B):

- **Local priority map**, where each subarea is associated with a priority level $\boldsymbol{c}_i \in$ {HIGH, MED, LOW} to represent costs incurred in case of location confusion.

- **Local frequency map**, where a visiting frequency level $\boldsymbol{\pi}_i \in \{\text{OFTEN, SOME, SELDOM}\}$ is indicated for each subregion.

where each level is given a nonnegative value to quantify the cost. Typical values are HIGH=3, MED=2, LOW=1, which also applies to the local frequency map.

The practicality of the nonuniform treatment of positioning accuracy is obvious. In an office building, most occupants will spend their time in their cubicles (HIGH cost of confusion, OFTEN frequency) and public areas such as conference rooms (MED, SOME) and kitchen (HIGH cost for energy apportionment, SOME) as compared to corridors (LOW, SELDOM). Another use case is the supermarkets, where the store manager might put HIGH value to food shelves to learn customer behaviors and LOW to open spaces. In the following, we formulate the problem in an optimization framework.

A. Optimization Framework

Our objective is to minimize the expected cost subject to router and fingerprints constraints, i.e., number/locations of routers/fingerprints:

$$\begin{aligned} \underset{\boldsymbol{\theta}}{\text{minimize}} \quad & \underset{Z\sim P_Z, X\sim P_{X|Z}}{\mathbb{E}}[L(Z, h_{\boldsymbol{\theta}}(X))|Z] \\ \text{subject to} \quad & \boldsymbol{\theta} = \{\boldsymbol{\theta}^{fp}, \boldsymbol{\theta}^{rt}\} \in \Theta \end{aligned} \tag{2}$$

where the expectation is with respect to $Z \sim P_Z$, the visiting probability given by the local frequency map, and $X \sim P_{X|Z}$, the fingerprints observation at location Z. To make the problem computationally tractable, we divide the space into N subregions, so the fingerprints decision variable $\boldsymbol{\theta}^{fp} \in \mathbb{N}_+^N$, $\mathbf{1}^\top \boldsymbol{\theta}^{fp} \leq N_{tot}$ where $\boldsymbol{\theta}_i^{fp}$ is the number of fingerprints collected at subregion i, and N_{tot} is the total number to be collected. As for the routers parameter, $\boldsymbol{\theta}^{rt}$, we allow the user to provide M locations to place the K routers (later we describe a heuristic of choosing the valuable router locations to lessen the computational burden).

The loss function $L(Z, h_{\boldsymbol{\theta}}(X))$ represents the cost of misclassification given the target is at location Z, i.e.,

$$L(Z, h_{\boldsymbol{\theta}}(X)) = \boldsymbol{c}_Z P_Z(h_{\boldsymbol{\theta}}(X) \neq Z), \tag{3}$$

where $\boldsymbol{c}_Z$ is indicated by the local priority map, and $h_{\boldsymbol{\theta}}(X)$ is the Bayes optimal classifier which in our case is the linear/quadratic discriminant analysis (LDA/QDA):

Linear/Quadratic Discriminant Analysis: Given two distributions $\mathcal{N}(\boldsymbol{\mu}_k, \Sigma_k)$, $k \in \{m, l\}$, for an observation $\boldsymbol{x}$, define the discriminant score for distribution k as $d_k(\boldsymbol{x}) = -\frac{1}{2}{\boldsymbol{x}_m}^\top \Sigma_k^{-1} \boldsymbol{x}_m + \boldsymbol{\mu}_k^\top \Sigma_k^{-1} \boldsymbol{x} - \frac{1}{2}\boldsymbol{\mu}_k^\top \Sigma_k^{-1} \boldsymbol{\mu}_k + \ln(\boldsymbol{\pi}_k) - \frac{1}{2}\ln|\Sigma_k|$, the optimal classification rule is given by

$$h(\boldsymbol{x}) = \arg\max_k d_k(\boldsymbol{x}) \tag{4}$$

For distinct covariance matrices, $\Sigma_m \neq \Sigma_l$, the above classification is known as Quadratic Discriminant Analysis (QDA). If the covariances are equal, the discriminant score can be simplified as $d_k(\boldsymbol{x}) = \boldsymbol{\mu}_k^\top \Sigma_k^{-1} \boldsymbol{x} - \frac{1}{2}\boldsymbol{\mu}_k^\top \Sigma_k^{-1} \boldsymbol{\mu}_k + \ln(\boldsymbol{\pi}_k)$, and the corresponding classifier becomes Linear Discriminant Analysis (LDA) [18]. Both QDA and LDA yield maximum posterior distribution, thus are reasonable classifers to employ for fingerprints-based positioning. In the following, we derive the analytic form of the misclassification rate in (3) to evaluate our objective function in (2) explicitly.

B. Theoretical Results for Misclassification Rate

Assume that the true class of $\boldsymbol{x}$ is m, i.e., $\boldsymbol{x}_m \sim \mathcal{N}(\boldsymbol{\mu}_m, \Sigma_m)$, then we will have misclassification if:

$$d_m(\boldsymbol{x}_m) < d_l(\boldsymbol{x}_m) \tag{5}$$

between two classes m and l. In the following, we consider the cases for the LDA and QDA based on the relation of covariance matrices.

*1) **LDA** [19]:* For $\Sigma_m = \Sigma_l$, (5) is equivalent to:

$$\boldsymbol{v}_{ml}^\top \boldsymbol{x}_m + a_{ml} < 0 \tag{6}$$

where $a_{ml} = -\frac{1}{2}\left(\boldsymbol{\mu}_m^\top \Sigma_m^{-1} \boldsymbol{\mu}_m - \boldsymbol{\mu}_l^\top \Sigma_l^{-1} \boldsymbol{\mu}_l\right) + \ln\frac{\boldsymbol{\pi}_m}{\boldsymbol{\pi}_l}$, $\boldsymbol{v}_{ml} = \Sigma_m^{-1}(\boldsymbol{\mu}_m - \boldsymbol{\mu}_l)$. Since $\boldsymbol{x}_m \sim \mathcal{N}(\boldsymbol{\mu}_m, \Sigma_m)$, we have

$$\underbrace{P\left(\boldsymbol{v}_{ml}^\top \boldsymbol{x}_m + a_{ml} < 0\right)}_{P_m(h(\boldsymbol{x})\neq m)} = \Phi\left(-\frac{\boldsymbol{v}_{ml}^\top \boldsymbol{\mu}_m + a_{ml}}{\boldsymbol{v}_{ml}^\top \Sigma_m \boldsymbol{v}_{ml}}\right), \tag{7}$$

where $\Phi(\cdot)$ is the cumulative distribution function for standard Gaussian variable $\mathcal{N}(0, 1)$.

*2) **QDA** :* Inspired by the drivation of misclassification rate for LDA [19], for $\Sigma_m \prec \Sigma_l$ (the case of $\Sigma_m \succ \Sigma_l$ is similar), condition (5) is equivalent to

$$-\tfrac{1}{2}{\boldsymbol{x}_m}^\top \Sigma_{ml} \boldsymbol{x}_m + \boldsymbol{v}_{ml}^\top \boldsymbol{x}_m + a_{ml} < 0 \tag{8}$$

where $\Sigma_{ml} = \Sigma_m^{-1} - \Sigma_l^{-1}$, $\boldsymbol{v}_{ml} = \Sigma_m^{-1}\boldsymbol{\mu}_m - \Sigma_l^{-1}\boldsymbol{\mu}_l$, $a_{ml} = -\frac{1}{2}\left(\boldsymbol{\mu}_m^\top \Sigma_m^{-1} \boldsymbol{\mu}_m - \boldsymbol{\mu}_l^\top \Sigma_l^{-1} \boldsymbol{\mu}_l\right) + \ln\frac{\boldsymbol{\pi}_m |\Sigma_l|^{1/2}}{\boldsymbol{\pi}_l |\Sigma_m|^{1/2}}$. We can rewrite the left hand side term as follows:

$$\begin{aligned} & -\tfrac{1}{2}{\boldsymbol{x}_m}^\top \Sigma_{ml} \boldsymbol{x}_m + \boldsymbol{v}_{ml}^\top \boldsymbol{x}_m + a_{ml} \\ &= -\tfrac{1}{2}\left\|\Sigma_{ml}^{1/2}\boldsymbol{x}_m - \underbrace{\Sigma_{ml}^{-1/2}\boldsymbol{v}_{ml}}_{\boldsymbol{\omega}_{ml}}\right\|_2^2 + a_{ml} + \tfrac{1}{2}\boldsymbol{v}_{ml}^\top \Sigma_{ml}^{-1}\boldsymbol{v}_{ml} \\ &= -\tfrac{1}{2}\sum_{i=1}^K \left(s_{ml}^{1/2}[\boldsymbol{x}_m]_i - [\boldsymbol{\omega}_{ml}]_i\right)^2 + a_{ml} + \tfrac{1}{2}\boldsymbol{v}_{ml}^\top \Sigma_{ml}^{-1}\boldsymbol{v}_{ml} \end{aligned}$$

where $[\boldsymbol{x}]_i$ is the i-th component of $\boldsymbol{x}$. Since in our formulation, Σ_{ml} is diagonal matrix with identical diagnoal entries s_{ml} for $i \in [K]$, we can see that $Y^{(m)} = \frac{1}{s_{ml}\sigma_m^2}\sum_{i=1}^K \left(s_{ml}^{1/2}[\boldsymbol{x}_m]_i - [\boldsymbol{\omega}_{ml}]_i\right)^2$ is a noncentral chi-squared distribution with the degrees of freedom K and noncentrality parameter $\lambda^{(ml)} = \sum_{i=1}^K \left(\frac{s_{ml}^{1/2}[\boldsymbol{\mu}_m]_i - [\boldsymbol{\omega}_{ml}]_i}{s_{ml}^{1/2}\sigma_m}\right)^2$. Thus the probability of misclassification given that the true class is m is given by:

$$P_m(h(\boldsymbol{x}) \neq m) = 1 - F\left(\frac{\boldsymbol{v}_{ml}^\top \Sigma_{ml}^{-1}\boldsymbol{v}_{ml} + 2a_{ml}}{s_{ml}\sigma_m^2}; K, \lambda^{(ml)}\right), \tag{9}$$

where $F(\cdot; k, \lambda)$ is the cumulative distribution function of the noncentral chi-squared distribution with degrees K and noncentrality parameter λ.

Applications to APEC: The gist of APEC is to select the number of fingerprints and placement of routers so that the location misclassification rate weighted by the priority and visiting frequency is minimized. Intuitively, the more fingerprints $\boldsymbol{x}_i^{(t)}$ collected the better we can estimate the mean at that location $\Lambda_{i,\cdot}^\top$ and the less the misclassification rate (refer Section II.B for the relations). By the maximum

likelihood method, our estimates of $\Lambda_{i,\cdot}^{\top}$ is the sample mean of fingerprints $\boldsymbol{x}_i^{(t)}$, which is normally distributed with mean $\Lambda_{i,\cdot}^{\top}$ and covariance $\frac{1}{n_i}\tilde{\Sigma}_i$, where n_i is the number of fingerprints collected. By *Assumption 1*, $\tilde{\Sigma}_i$ is the same for all locations $i \in [N]$. Consider m and l to be neighboring two regions, then by applying the results in (7) and (9) with $\Sigma_m = \frac{1}{n_m}\tilde{\Sigma}$ and $\Sigma_l = \frac{1}{n_l}\tilde{\Sigma}$ ($\tilde{\Sigma}$ is diagonal with entries $\tilde{\sigma}^2$ by *Assumption 1*),

$$P_m(h(\boldsymbol{x}) \neq m) = \begin{cases} \Phi\left(-\frac{\boldsymbol{v}_{ml}^{\top}\boldsymbol{\mu}_m + a_{ml}}{\sqrt{\frac{1}{n_m}\boldsymbol{v}_{ml}^{\top}\tilde{\Sigma}\boldsymbol{v}_{ml}}}\right), & n_m = n_l \\ 1 - F\left(\frac{\boldsymbol{v}_{ml}^{\top}\Sigma_{ml}^{-1}\boldsymbol{v}_{ml} + 2a_{ml}}{s_{ml}\sigma_m^2}; K, \lambda_1^{(ml)}\right), & n_m > n_l \\ F\left(\frac{\boldsymbol{v}_{ml}^{\top}\Sigma_{ml}^{-1}\boldsymbol{v}_{ml} - 2a_{ml}}{s_{ml}\sigma_m^2}; K, \lambda_2^{(ml)}\right), & n_m < n_l \end{cases} \tag{10}$$

where $\boldsymbol{v}_{ml} = \tilde{\Sigma}^{-1}(n_m\boldsymbol{\mu}_m - n_l\boldsymbol{\mu}_l)$, $\Sigma_{ml} = |n_m - n_l|\tilde{\Sigma}^{-1}$, $s_{ml} = |n_m - n_l|\,\tilde{\sigma}^{-2}$, $a_{ml} = -\frac{1}{2}\left(n_m\boldsymbol{\mu}_m^{\top}\tilde{\Sigma}^{-1}\boldsymbol{\mu}_m - n_l\boldsymbol{\mu}_l^{\top}\tilde{\Sigma}^{-1}\boldsymbol{\mu}_l\right) + \ln\frac{\boldsymbol{\pi}_m n_m^{K/2}}{\boldsymbol{\pi}_l n_l^{K/2}}$, $\boldsymbol{\omega}_{ml} = \Sigma_{ml}^{-1/2}\boldsymbol{v}_{ml}$, σ_m^2 is the diagonal element of $\frac{1}{n_m}\tilde{\Sigma}$, and the noncentrality parameters $\lambda_1^{(ml)} = \sum_{i=1}^{K}\left(\frac{s_{ml}^{1/2}[\boldsymbol{\mu}_m]_i - [\boldsymbol{\omega}_{ml}]_i}{s_{ml}^{1/2}\sigma_m}\right)^2$, $\lambda_2^{(ml)} = \sum_{i=1}^{K}\left(\frac{s_{ml}^{1/2}[\boldsymbol{\mu}_m]_i + [\boldsymbol{\omega}_{ml}]_i}{s_{ml}^{1/2}\sigma_m}\right)^2$. The above formula ties the HBSM model and optimization framework to allow us evaluate the objective function efficiently. Now, we introduce the APEC algorithm.

C. APEC Algorithm

We can write out the expected loss in (2) as follow:

$$\mathop{\mathbb{E}}_{\substack{Z\sim P_Z,\\ X\sim P_{X|Z}}} L(Z, h_{\boldsymbol{\theta}}(X)) = \sum_{i\in[N]} \boldsymbol{\pi}_i \underbrace{\sum_{j\in R(i)} \boldsymbol{c}_i P_i(h_{\boldsymbol{\theta}}(\boldsymbol{x}) = j)}_{\text{Weighted cost of location confusion}}, \tag{11}$$

where $\boldsymbol{\pi}_i$ is the visiting frequency (normalized from the local frequency map), $\boldsymbol{c}_i$ is the location confusion coefficient given by the local priority map, $R(i)$ is the neighborhood of point i. APEC optimizes over the following parameters:

- $\boldsymbol{\theta}^{rt}$ (router locations): Given M possible locations, choose K to place the routers.
- $\boldsymbol{\theta}^{fp}$ (fingerprints): Plan the number of fingerprints to be collected at each subregion $i \in [N]$ such that $\boldsymbol{\theta}^{fp} = [n_1, \cdots, n_N]^{\top} \in \mathbb{N}_+^N$, $\mathbf{1}^{\top}\boldsymbol{\theta}^{fp} \leq N_{tot}$.

It can be seen that the problem is combinatorial in nature, which requires integer programming. The computation is formidable for large scale problems. For instance, there are $\binom{N + N_{tot} - 1}{N - 1}$ possible solutions to distribute N_{tot} fingerprints to N subregions. APEC Greedy, therefore, is proposed to solve the problem efficiently, as shown in Algorithm 1, which is based on the HBSM (*line 5*, see Section II) and weighted misclassification cost (*line 8*, see Section III).

The APEC Greedy algorithm exhaustively searches for router locations ($\boldsymbol{\theta}^{rt} \in S^{rt}$, where S^{rt} is all possible combinations of M choose K locations, *line 1*), and stochastically optimizes for fingerprints vectors $\boldsymbol{\theta}^{fp}$. The asymptotic case

Algorithm 1: Pseudo-code of APEC Greedy

`APEC_Greedy(`Maps, N_{tot}, K`)`
Input: Maps: possible M locations to place K routers (S^{rt}), centers of N subregions to collect N_{tot} fingerprints (S^{fp}), local priority/frequency maps
Initialization:
1 $S^{rt} \leftarrow$ `Comb(`Maps, K`)` `// Set of router locations`
2 $b \leftarrow$ Number of fingerprints (fp) increment
3 $B \leftarrow$ Batch size
$\boldsymbol{\theta} \leftarrow \{\}$ `// Cell to store the history of` $\{\boldsymbol{\theta}^{fp}, \boldsymbol{\theta}^{rt}\}$
$V \leftarrow [\,]$ `// Vector to store the history of costs`
$bookInd \leftarrow 1$
Main program:
4 **for** $\boldsymbol{\theta}^{rt} \in S^{rt}$ **do** `// Scan possible router locations`
5 $\tilde{\Lambda}, \tilde{\Gamma}, \tilde{\Sigma} \leftarrow$ `HBSM(`$\boldsymbol{\theta}^{rt}, S^{fp}$`)` `// Sec.II`
$\boldsymbol{\theta}^{fp} \leftarrow \mathbf{1}(N, 1)$ `// Start with 1 fp per location`
$k \leftarrow N$ `// Current number of fps`
while $k < N_{tot}$ **do**
$\boldsymbol{\theta}_t \leftarrow \{\}$, $V_t \leftarrow [\,]$
for $i \in \{1, ..., B\}$ **do**
`/* Randomly choose` b `indices out of` N `with replacement, then increment the corresponding entries in` $\hat{\boldsymbol{\theta}}^{fp}$ `*/`
6 $\boldsymbol{u} \leftarrow$ `RandInd(`N, b`)`
7 $\hat{\boldsymbol{\theta}}^{fp} \leftarrow \boldsymbol{\theta}^{fp}$, $\hat{\boldsymbol{\theta}}^{fp}_{\boldsymbol{u}} \leftarrow \hat{\boldsymbol{\theta}}^{fp}_{\boldsymbol{u}} + 1$
8 $v \leftarrow \mathop{\mathbb{E}}_{Z,X} L(Z, h_{\boldsymbol{\theta}}(X))$ `// Equ. (11)`
$\boldsymbol{\theta}_t(i) \leftarrow \hat{\boldsymbol{\theta}}^{fp}$, $V_t(i) \leftarrow v$
$i_{bst} \leftarrow \arg\min_i V_t(i)$
$\boldsymbol{\theta}^{fp} \leftarrow \boldsymbol{\theta}_t(i_{bst})$, $v_{bst} \leftarrow V_t(i_{bst})$
$k \leftarrow k + b$ `// Increment fps by stepsize`
$\boldsymbol{\theta}(bookInd) \leftarrow \{\boldsymbol{\theta}^{fp}, \boldsymbol{\theta}^{rt}\}$, $V(bookInd) \leftarrow v_{bst}$
$bookInd \leftarrow bookInd + 1$
9 $i_{bst} \leftarrow \arg\min_i V(i)$
$\{\boldsymbol{\theta}^{rt}_{bst}, \boldsymbol{\theta}^{fp}_{bst}\} \leftarrow \boldsymbol{\theta}(i_{bst})$
Output: $\{\boldsymbol{\theta}^{rt}_{bst}, \boldsymbol{\theta}^{fp}_{bst}\}$ `// APEC Greedy solution`

of choosing $b = N_{tot}$ and batch size $B \to \infty$ (*lines 2,3*) produces the same result of exhaustive search at the cost of infeasible computation time. The simulation experiments in the following verifies that APEC Greedy performs almost as well as exhaustive search at computational advantage. We also propose heuristics in selecting the most useful locations to place routers through router-fingerprints decoupling to resolve scalability issue in field deployment.

IV. Experimental Results

A. Toy Case Study

Through the simulation, we compare the performance of APEC Greedy with APEC Exhaustive, and understand the router and fingerprints placement in relation to the local priority and frequency maps. Specifically, we will examine the following heuristics that APEC Greedy (Algorithm 1) employs to reduce computational complexity:

- **Heuristic 1 (Coordinate Descent)**: Fingerprints budget is allocated in $\boldsymbol{\theta}^{fp}$ by random selection of location candidates (*lines 6,7*) and choosing the set that makes the most cost reduction (*line 9*).
- **Heuristic 2 (Router-Fingerprints Decoupling)**: The set of optimal router locations S^{rt} that minimizes the

loss (11) is chosen by assuming a uniform allocation of fingerprints budget, i.e., each spot has fingerprints $\frac{N_{tot}}{N}$. Then, the fingerprints $\boldsymbol{\theta}^{fp}$ are optimized within the reduced set (*line 4*) instead of the full set with combinatorial number of router candidates.

We design a simple problem as shown in Figure 1 with $M = 9$ possible router locations and $N = 5$ subregions, where the location priority is color coded, and the frequency is identical for all 5 subregions. . The total number of fingerprints N_{tot} is restricted so that APEC Exhaust is tractable. A random approach is also implemented where the fingerprints are distributed randomly.

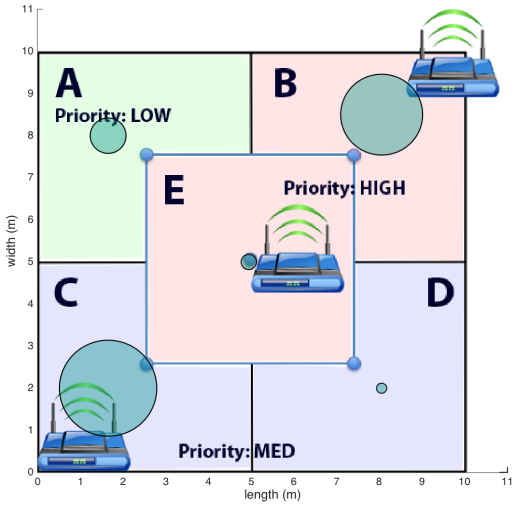

Figure 1. Map of the toy example showing the access points locations and fingerprints allocations (radius of the green circle) determined by APEC Exhaust (also APEC Greedy since they agree).

1) Examination of Heuristic 1: The losses (8) of fingerprints allocation $\boldsymbol{\theta}^{fp}$ given by APEC Exhaust, Greedy, and random approach corresponding to each router configuration is shown in Figure 2. The router setup is indexed by the expected loss of APEC Exhaust, so ideally other methods should incur similar loss and exhibit descending trend to match the optimal solution.

2) Examination of Heuristic 2: The router-fingerprints decoupling heuristic makes a trade-off between cost and computation by sequentially optimizing over $\boldsymbol{\theta}^{rt}$ and $\boldsymbol{\theta}^{fp}$ in problem (2), which brings computational advantage for large-scale problems. Even though the heuristic relies on estimation of the optimal cost that is not the most accurate, the performance is guaranteed if the estimation preserves rankings among the candidates, so that the best router setups are revealed nevertheless, as shown in Figure 3. As can be seen, though the estimation is noisy, the decoupling heuristic can recover the best 20 router setups with high probability, which is not likely for the random selection approach.

Another possible heuristic, *random selection*, is to treat each setup uniformly, where they have identical distribution of expected loss, as shown in Figure 3. We might end up in a region, i.e., the right half of the graph, where even with the optimized fingerprints $\boldsymbol{\theta}^{fp}_{*}$ the incurred loss is significantly

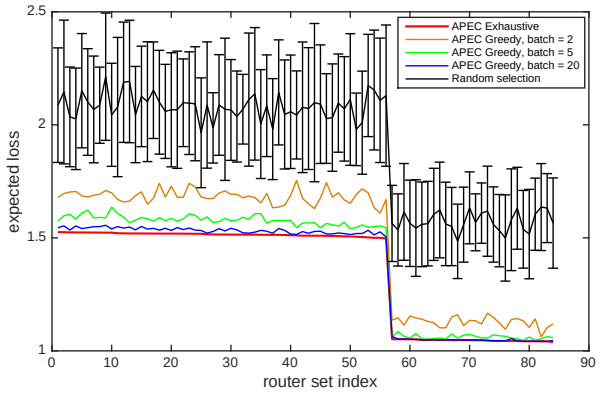

Figure 2. Expected loss of fingerprints allocation $\boldsymbol{\theta}^{fp}$ for each router setup (out of 84 candidates) with $N_{tot} = 15$ total budget, $N = 5$ subregions, $K = 3$ routers, as selected by APEC Exhaust, APEC Greedy (with different batch sizes B), and random approach (black error bar showing mean$\pm$1 standard deviation over 20 test runs).

higher then the optimal, since unlike the decoupling heuristic, the ranking information is lost.

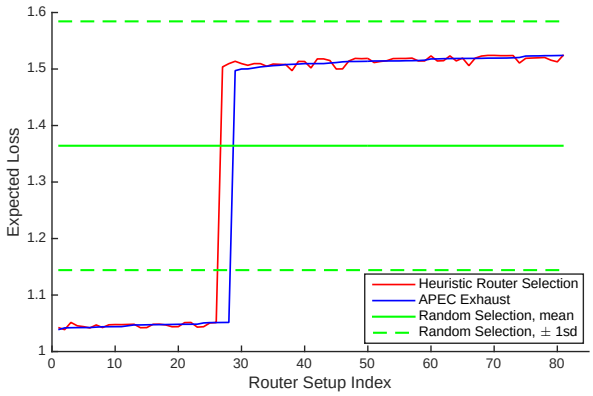

Figure 3. Expected loss vs. router setup indexed by the optimal costs given by solving the fully coupled problem (APEC Exhaust). The plot also shows the loss estimated by random selection (green, mean $\pm$ 1 standard deviation) and heuristic router selection (red).

B. Field Deployment

The theoretical foundation of APEC Greedy, a method to predetermine the optimal router locations and fingerprints allocation for indoor positioning system (IPS), is the formulation of the optimization problem (2), which takes into account the hierarchical Bayesian signal model (HBSM, see Section II), location priority, and visiting frequencies. As most fingerprinting system employs methods such as K-Nearest Neighbor (KNN) for positioning [1], the assessment of APEC requires the examination of the following:

- **Hypothesis 1 (Objective Consistency)**: Given $(\boldsymbol{\theta}^{rt}, \boldsymbol{\theta}^{fp})$, the expected loss given in (11) is a good indicator of the actual loss of the system. *Objective consistency* ensures that the solution of (2) is (near-) optimal in practice (see Figure 5).

TABLE II. SUMMARY OF DATA COLLECTED IN EXPERIMENT A (WITH 5 ROUTERS) AND B (7 ROUTERS) FOR THREE DEVICES (IPHONE, IPAD, ANDROID).

	iPhone	iPad	Android
Exp A: 7 RTs	Avg: 72±18 pts Tot: 144 minutes	Avg: 72±15 pts Tot: 144 minutes	Avg: 96±25 pts Tot: 193 minutes
Exp B: 9 RTs	Avg: 84±17 pts Tot: 167 minutes	Avg: 80±19 pts Tot: 160 minutes	Avg: 98±12 pts Tot: 196 minutes

- **Hypothesis 2 (Solution Superiority)**: Though the objective consistency if met can guarantee optimal solution, we still want to verify that APEC, with the application of heuristics proposed in Section IV-A, performs well with respect to the actual cost (Figure 6).

Data collection takes place in the Center for Research in Energy Systems Transformation (CREST) on the UC Berkeley campus, where Figure 7 shows the floor plan and location priority. The priority is set HIGH to facilitate region-based thermal and lighting control [20], MEDIUM for shared spaces such as kitchen and conference room for energy apportionment, and LOW for corridors. Fingerprints are collected by an Android phone (Nexus 5), iPad, and iPhone, in two independent experiments, where 7 or 9 access points (D-Link DIR-605LWiFi Cloud Router) are installed as summarized in Table II. The average number of fingerprints $\pm$ 1 standard deviation for all 40 subregions ("Avg"), and the total time for the experiment, which accounts for roughly 3 seconds required to collect one fingerprint ("Tot") are indicated in the table.

Figure 4 shows the RSSI with respect to the log distance from the fingerprint to the access point. Generally, a linear relation is observed (with correlation score .77), though the variance can be reduced by accounting for walls as suggested in [1]. It can be seen that the dependency is stable for all devices (Android, iPad, iPhone), which ensures cross-platform performance of fingerprints configuration.

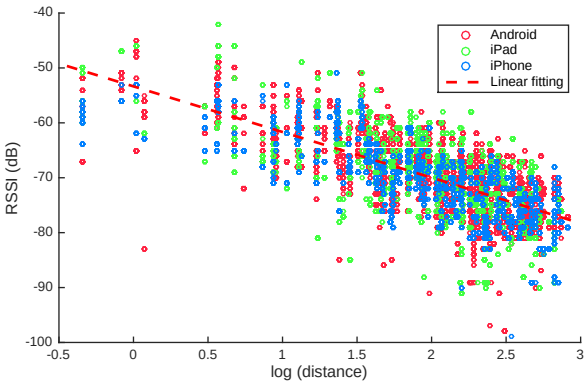

Figure 4. Plots of RSSI vs. log distance color coded by devices. A linear regression line is fitted on the data: $\text{RSSI} = -8.31 \cdot \log(d) - 53.4$.

1) Examination of Objective Consistency: Given location priority map $\boldsymbol{c}$ and frequency map $\boldsymbol{\pi}$, the actual loss of an IPS system parameterized by $(\boldsymbol{\theta}^{rt}, \boldsymbol{\theta}^{fp})$ is given by

$$\hat{L}(\boldsymbol{\theta}^{rt}, \boldsymbol{\theta}^{fp}) = \sum_{i \in [N]} \boldsymbol{\pi}_i \underbrace{\sum_{j \in R(i)} \boldsymbol{c}_i \xi_i(j)}_{\text{Weighted cost of location confusion}}, \tag{12}$$

where $\xi_i(j)$ is the empirical evaluation of the misclassification rate of location i to its neighboring spots j,

$$\xi_i(j) = \frac{1}{|\mathcal{X}_i|} \sum_{\boldsymbol{x} \in \mathcal{X}_i} \mathbb{1}(h_{\boldsymbol{\theta}}(\boldsymbol{x}) = j, j \neq i). \tag{13}$$

$\mathcal{X}_i$ is the set of test points at location i, and $\mathbb{1}(h_{\boldsymbol{\theta}}(\boldsymbol{x}) = j, j \neq i)$ is the indicator function valued 1 if the IPS function $h_{\boldsymbol{\theta}}(\boldsymbol{x})$, e.g., 1-nearest neighbor, outputs $j \neq i$, and 0 otherwise. Given a particular setup, the actual cost and the expected cost given in (11) is shown in Figure 5.

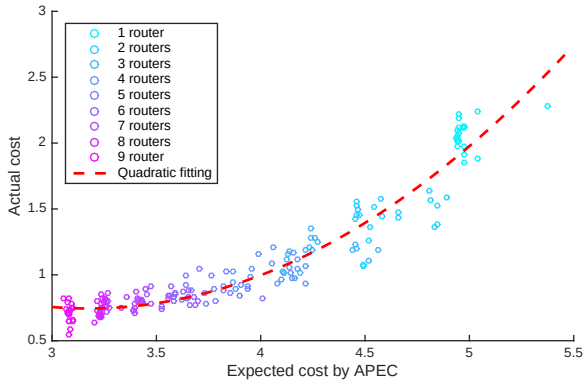

Figure 5. Plots of the actual cost (12) vs. the expected cost (11), color coded by the number of routers deployed. A quadratic curve is fitted to the data: $\hat{L} = 0.37 \cdot L_e^2 - 2.34 \cdot L_e + 4.46$, where $\hat{L}$ and L_e are actual and expected losses given in (12) and (11) respectively.

As can be seen, the expected cost by APEC is a strong indicator of the actual cost of IPS. Compared to $\xi_i(j)$ which is hard to determine *a priori*, the expected cost is easy to calculate as a function of $(\boldsymbol{\theta}^{rt}, \boldsymbol{\theta}^{fp})$, as a closed form solution of the misclassification rate $P_i(h_{\boldsymbol{\theta}}(\boldsymbol{x}) = j)$ is derived in (10). In other words, *we can predict the fingerprints-based IPS performance based on the router-fingerprints configuration*, which can be useful for other problems as well, such as the optimization of the number of routers to be deployed under budget constraints.

2) Examination of Solution Superiority: Though it is difficult to check strict optimality due to the non-convexity and intractable state space of the problem, solution superiority can be demonstrated by comparing to the two common practices, i.e., *random* and *uniform* selections, where the former randomly allocates fingerprints, the latter maintains a balanced profile over the space. Both methods, nevertheless, ignores user preferences encoded in the location priority and frequency maps. As the expected cost is shown to be a strong predictor of the actual cost, APEC, theoretically, can reach a *preferred* solution as guided by the optimization of (2).

As is shown in Figure 6, which illustrates the distribution of actual costs (12) in Experiment A and B (see Table II), the strategy suggested by APEC performs better than the

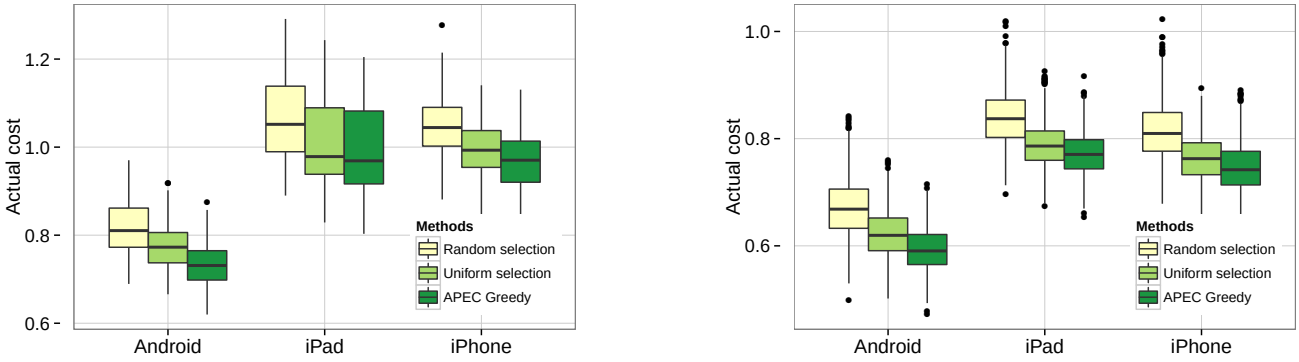

Figure 6. Actual cost distribution in Experiment A (left) and B (right) for all devices color coded by the fingerprinting methods, i.e., random selection, uniform selection, and APEC Greedy. The box goes from the 1^{st} quantile to the 3^{rd} quantile, with the black line indicating the mean. As a side note, Android device incurs less cost in both experiments as a result of its stability of the RSSI signal.

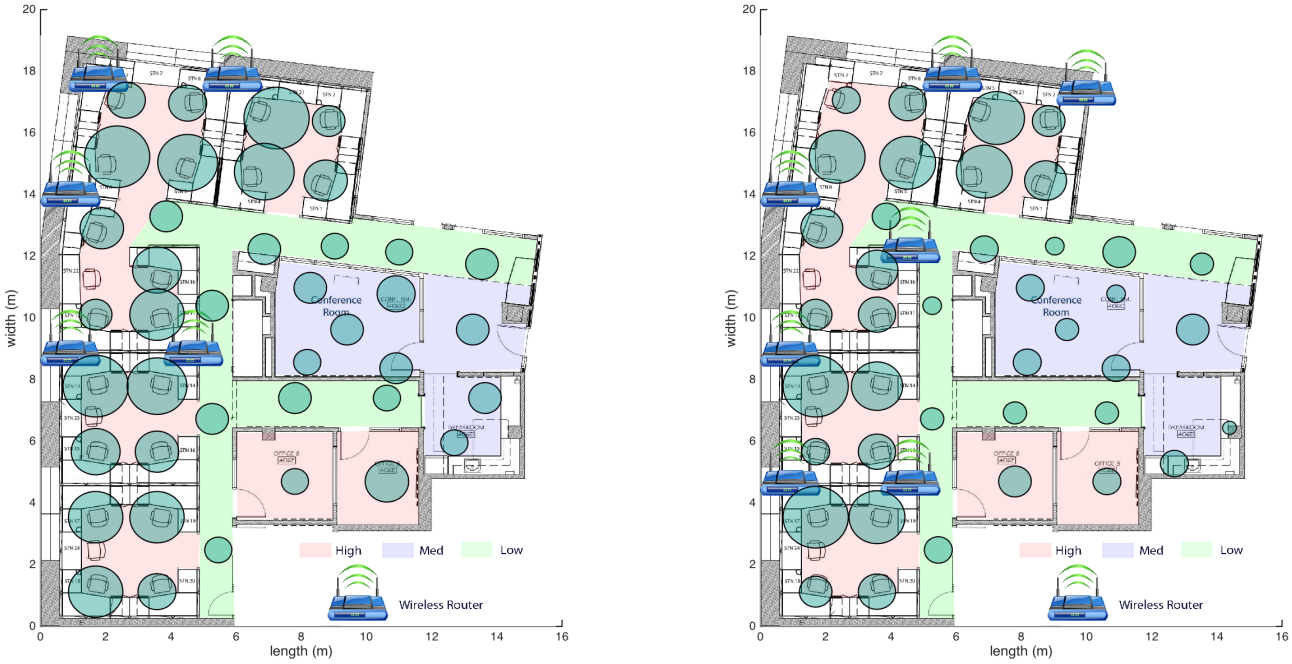

Figure 7. Visualization of IPS configuration in CREST for experiment A (left) and B (right), where 5 or 7 access points are deployed according to APEC Greedy. Location priority map is color coded as illustrated in the legend. Location frequency map is not shown, which is HIGH for cubicles, MED for shared spaces, and LOW for corridors. The radius of the green circle indicates the number of fingerprints at the spot.

others for all devices. Since a lower actual cost is a result of accurate classification in high priority areas, APEC is effective in catering to user needs.

3) Visualization: The best fingerprints configuration, $(\boldsymbol{\theta}^{rt}, \boldsymbol{\theta}^{fp})$, as chosen by APEC Greedy for Experiment A and B are shown in Figure 7. Some simple guiding rules can be learned from observations:

- Routers are placed in regions with high priority to ensure fingerprints distinction.
- More fingerprints are needed for high priority areas.
- Region close to the routers require more fingerprints.

The third point, though less intuitive, can be explained by inspecting Figure 4, where the RSSI changes slowly in near-router regions, and the difference of distances are not sufficient for fingerprints separations.

As future work, we would like to implement the visualization in mobile platforms to further assist planning when fingerprints IPS is in demand.

V. Conclusion

APEC systematically optimizes the locations of access points and allocations of fingerprints over space by taking into consideration user preferences through local priority/frequency maps and budget constraints, which can be combined with

existing fingerprinting-based methods to improve utility of the indoor positioning system.

The core of APEC is the optimization problem (2), where the objective is the expected loss (11) based on the proposed HBSM and theoretical results on the misclassification rates. As verified by *objective consistency* (Figure 5), the expected loss is a strong predictor for the actual loss incurred by the IPS system, a useful result to determine the performance of the system in the planning stage.

To make APEC computationally tractable, the coordinate descent and router-fingerprints decoupling heuristics are proprosed, which are validated by simulation. Experiments with three devices (Android, iPad, iPhone) in two different setups (7/9 routers) demonstrates *solution superiority* of APEC as compared to the uniform and random approaches. Through visualization several simple rules are developed, while the map serves as a visual guidance for field deployment. As future work we want to implement and visualize APEC configuration on mobile platforms to facilitate regular planning.

ACKNOWLEDGMENT

This research is funded by the Republic of Singapore's National Research Foundation through a grant to the Berkeley Education Alliance for Research in Singapore (BEARS) for the Singapore-Berkeley Building Efficiency and Sustainability in the Tropics (SinBerBEST) Program. BEARS has been established by the University of California, Berkeley as a center for intellectual excellence in research and education in Singapore.

REFERENCES

[1] P. Bahl and V. N. Padmanabhan, "Radar: An in-building rf-based user location and tracking system," in INFOCOM 2000. Nineteenth Annual Joint Conference of the IEEE Computer and Communications Societies. Proceedings. IEEE, vol. 2. Ieee, 2000, pp. 775–784.

[2] T. Roos, P. Myllymki, H. Tirri, P. Misikangas, and J. Sievnen, "A probabilistic approach to wlan user location estimation," International Journal of Wireless Information Networks, vol. 9, 2002, pp. 155–164.

[3] M. Youssef and A. Agrawala, "The horus wlan location determination system," in Proceedings of the 3rd international conference on Mobile systems, applications, and services. ACM, 2005, pp. 205–218.

[4] Z. Yang, C. Wu, and Y. Liu, "Locating in fingerprint space: wireless indoor localization with little human intervention," in Proceedings of the 18th annual international conference on Mobile computing and networking. ACM, 2012, pp. 269–280.

[5] A. Rai, K. K. Chintalapudi, V. N. Padmanabhan, and R. Sen, "Zee: zero-effort crowdsourcing for indoor localization," in Proceedings of the 18th annual international conference on Mobile computing and networking. ACM, 2012, pp. 293–304.

[6] H. Liu, Y. Gan, J. Yang, S. Sidhom, Y. Wang, Y. Chen, and F. Ye, "Push the limit of wifi based localization for smartphones," in Proceedings of the 18th annual international conference on Mobile computing and networking. ACM, 2012, pp. 305–316.

[7] J.-g. Park, B. Charrow, D. Curtis, J. Battat, E. Minkov, J. Hicks, S. Teller, and J. Ledlie, "Growing an organic indoor location system," in Proceedings of the 8th international conference on Mobile systems, applications, and services. ACM, 2010, pp. 271–284.

[8] K. Chintalapudi, A. Padmanabha Iyer, and V. N. Padmanabhan, "Indoor localization without the pain," in Proceedings of the sixteenth annual international conference on Mobile computing and networking. ACM, 2010, pp. 173–184.

[9] H. Lim, L.-C. Kung, J. C. Hou, and H. Luo, "Zero-configuration indoor localization over ieee 802.11 wireless infrastructure," Wireless Networks, vol. 16, 2010, pp. 405–420.

[10] Y. Ji, S. Biaz, S. Pandey, and P. Agrawal, "Ariadne: a dynamic indoor signal map construction and localization system," in Proceedings of the 4th international conference on Mobile systems, applications and services. ACM, 2006, pp. 151–164.

[11] Y. Gwon and R. Jain, "Error characteristics and calibration-free techniques for wireless lan-based location estimation," in Proceedings of the second international workshop on Mobility management & wireless access protocols. ACM, 2004, pp. 2–9.

[12] D. Roland, E. Martin, and B. Robert, "Indoor navigation by wlan location fingerprinting," in UBICOMM, 2013, pp. 1–6.

[13] L. Li, G. Shen, C. Zhao, T. Moscibroda, J.-H. Lin, and F. Zhao, "Experiencing and handling the diversity in data density and environmental locality in an indoor positioning service," in Proceedings of the 20th annual international conference on Mobile computing and networking. ACM, 2014, pp. 459–470.

[14] J. Baxter, "A bayesian/information theoretic model of learning to learn via multiple task sampling," Machine Learning, vol. 28, no. 1, 1997, pp. 7–39.

[15] S.-T. Sheu, Y.-M. Hsu, and H.-Y. Chen, "Indoor location estimation using smart antenna system with virtual fingerprint construction scheme," in UBICOMM 2014, The Eighth International Conference on Mobile Ubiquitous Computing, Systems, Services and Technologies, 2014, pp. 281–286.

[16] H. D. Nguyen, T. M. Doan, and N. T. Nguyen, "Cgsil: A viable training-free wi-fi localization," in UBICOMM 2014, The Eighth International Conference on Mobile Ubiquitous Computing, Systems, Services and Technologies, 2014, pp. 268–274.

[17] C. E. Rasmussen, "Gaussian processes for machine learning," 2006.

[18] G. McLachlan, Discriminant analysis and statistical pattern recognition. John Wiley & Sons, 2004, vol. 544.

[19] B. Klaus, "Effect size estimation and misclassification rate based variable selection in linear discriminant analysi," Journal of Data Scienceg, vol. 11, 2013, p. 537.

[20] L. J. Ratliff, M. Jin, I. C. Konstantakopoulos, C. Spanos, and S. S. Sastry, "Social game for building energy efficiency: Incentive design," in 52nd Annual Allerton Conference on Communication, Control, and Computing, 2014, 2014.